Regulation of maternal phospholipid composition and IP_3-dependent embryonic membrane dynamics by a specific fatty acid metabolic event in *C. elegans*

Marina Kniazeva, Huali Shen, Tetyana Euler, Chen Wang, and Min Han[1]

Howard Hughes Medical Institute, Department of Molecular, Cellular, and Developmental Biology, University of Colorado, Boulder, Colorado 80309, USA

Natural fatty acids (FAs) exhibit vast structural diversity, but the functional importance of FA variations and the mechanism by which they contribute to a healthy lipid composition in animals remain largely unexplored. A large family of acyl-CoA synthetases (ACSs) regulates FA metabolism by esterifying FA to coenyzme A. However, little is known about how particular FA–ACS combinations affect lipid composition and specific cellular functions. We analyzed how the activity of ACS-1 on branched chain FA C17ISO impacts maternal lipid content, signal transduction, and development in *Caenorhabditis elegans* embryos. We show that expression of ACS-1 in the somatic gonad guides the incorporation of C17ISO into certain phospholipids and thus regulates the phospholipid composition in the zygote. Disrupting this ACS-1 function causes striking defects in complex membrane dynamics, including exocytosis and cytokinesis, leading to early embryonic lethality. These defects are suppressed by hyperactive IP_3 signaling, suggesting that C17ISO and ACS-1 functions are necessary for optimal IP_3 signaling essential for early embryogenesis. This study shows a novel role of branched chain FAs whose functions in humans and animals are unknown and uncovers a novel intercellular regulatory pathway linking a specific FA–ACS interaction to specific developmental events.

[*Keywords*: BCFA; branched chain fatty acid; acyl-CoA synthetase; somatic gonad; exocytosis; inositol trisphosphate]

Supplemental material is available for this article.

Received January 10, 2012; revised version accepted February 17, 2012.

Fatty acids (FAs) are highly diverse in their structure, and these structural variations contribute to the vast variety and complexity of higher-order lipids. Although the functional importance of FA variants in animal development and human health has been recognized by a limited number of studies using model organisms (e.g., Zhang et al. 2001; Kahn-Kirby et al. 2004; Kniazeva et al. 2008; Szafer-Glusman et al. 2008; Zuryn et al. 2010; Riquelme et al. 2011), mechanistic studies of how FA variants and numerous FA-modifying enzymes impact specific physiological functions are lacking. In a given organism, or even a given tissue, FA and lipid compositions are strictly regulated during development, but little is known about how it is accomplished. More specifically, zygotic lipids, like RNAs and proteins, are of maternal origin and are supplied during oogenesis. However, neither the functional importance nor the mechanism of achieving healthy lipid content in the zygote is known.

[1]Corresponding author.
E-mail mhan@colorado.edu.
Article is online at http://www.genesdev.org/cgi/doi/10.1101/gad.187054.112.

C17ISO, a monomethyl branched chain FA (mmBCFA) (Fig. 1A) present in many organisms from bacteria to humans, is involved in multiple processes in *Caenorhabditis elegans*, including initiation of post-embryonic development (Kniazeva et al. 2004, 2008; Entchev et al. 2008). A loss-of-function mutation in the mmBCFA-specific elongation enzyme ELO-5 causes a deficiency in C17ISO that results in early larval arrest and lethality. Dietary C17ISO, but not straight chain FAs, fully rescues the ELO-5-null mutants to wild-type growth and proliferation. ACS-1, a member of the acyl-CoA synthetase (ACS) enzyme family, is also required for C17ISO biosynthesis and therefore for viability of the animals (Kniazeva et al. 2008).

In general, ACSs catalyze esterification (or activation) of FAs to coenzyme A to form activated intermediates, which are substrates for elongation, degradation, or incorporation into complex lipids. ACS enzymes have been proposed to regulate lipid-related functions and homeostasis through this biochemical reaction (Mashek et al. 2007; Ellis et al. 2010). The conserved ACS family is encoded by a total of 22 predicted genes in *C. elegans* (26

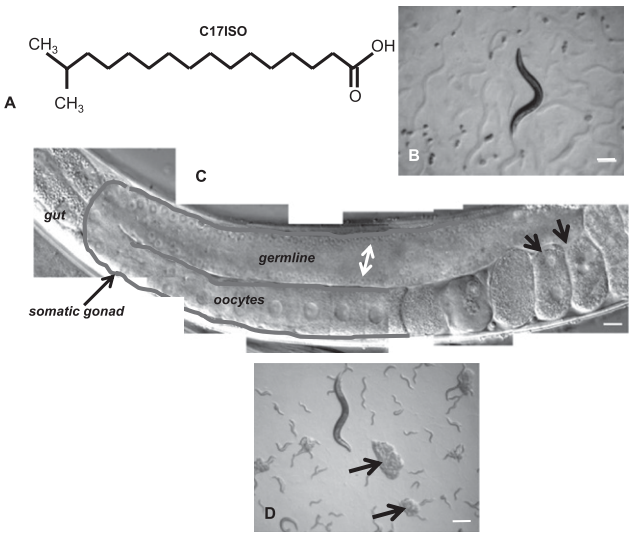

Figure 1. ACS-1 plays an essential role in embryogenesis. (*A*) Structure of mmBCFA C17ISO. (*B*) Dissecting microscope images showing that C17ISO added to the diet causes embryonic lethality in *acs-1(RNAi)* animals [termed *acs-1(RNAi)*^{C17ISO}]. Bar, 200 μm. (*C*) DIC image showing an *acs-1(RNAi)*^{C17ISO} animal. The double arrow marks the gonadal lumen (rachis) surrounded by the single layer of germline nuclei. The gray lines mark the somatic gonad wrapping around the germline. These apparently healthy adults produced only dead embryos (Emb). Small arrows point to two one-cell embryos with multiple nuclei (also see Fig. 3). Bar, 15 μm. (*D*) Dissecting microscope image showing the *acs-1(gk3066)* deletion mutants that have been rescued to continuous proliferation by a wild-type *acs-1* transgene [*acs-1(gk3066);Ex[acs-1(full)]*]. Arrows point to dead eggs on the plate. In this case, Emb resulted from a loss of the extra chromosomal array in the somatic gonad (see the Results; Fig. 2H–M).

in mammals), each potentially generating multiple proteins via alternative splicing (Mashek et al. 2007; Watkins et al. 2007; http://www.wormbase.org). It has been proposed that metabolic trafficking of each fatty acyl-CoA is determined by the ACS that esterifies the FA substrate (Coleman et al. 2002; Black and DiRusso 2007). It is conceivable that the production of a large number of ACSs accommodates the need for the diversification of lipid structures and functions. Since ACSs regulate FAs and lipid homeostasis, studying the specificity of FA–ACS interactions in living organisms is important for understanding their impact on cellular and organismic physiology and for the prevention and treatment of pathological conditions.

Here we report the discovery and analysis of an intriguing interaction between C17ISO and ACS-1 in *C. elegans* that takes place in the somatic gonad but subsequently regulates lipid composition and membrane dynamics essential for embryogenesis.

Results

ACS-1 and C17ISO play an essential role in early embryogenesis

We previously showed that ELO-5 and ACS-1 are essential enzymes in de novo synthesis of C17ISO and that C17ISO is indispensable for larval growth and development in *C. elegans*. RNAi inhibition of either *elo-5* or *acs-1* from the time of hatching causes early larval arrest and lethality, which can be rescued by including C17ISO in the diet (Kniazeva et al. 2004, 2008). We found that with C17ISO supplementation, *elo-5(RNAi)* animals proliferated indefinitely, while *acs-1(RNAi)* animals grew as wild type for only one generation and produced only dead embryos (Emb phenotype) (Fig. 1B,C). The combination of *acs-1(RNAi)* treatment with C17ISO supplement is hereafter termed *acs-1(RNAi)*^{C17ISO}. To exclude a possibility that the Emb phenotype of *acs-1(RNAi)*^{C17ISO} was due to a nonspecific silencing effect on a secondary target, we carried out several control experiments and found no evidence for nonspecific targeting of *acs-1(RNAi)* (Materials and Methods).

We also examined whether *acs-1(RNAi)*^{C17ISO} embryos remained deficient for C17ISO in the absence of *acs-1* expression by comparing the FA compositions of lipid extracts from wild-type and *acs-1(RNAi)*^{C17ISO} embryos using gas chromatography (GC). The GC data revealed the presence of C17ISO FA in the total lipid extracts from both samples (Supplemental Fig. S1), indicating that C17ISO could be delivered to embryos, in one form or another, in the absence of *acs-1* expression.

We then examined whether the Emb phenotype is associated with an *acs-1* deletion mutant [*acs-1(gk3066)*]. Because homozygous *acs-1(gk3066)* animals are larval-lethal, we generated a transgenic strain, *acs-1(gk3066); Ex[acs-1(full)]*, that expressed an extra chromosomal array carrying wild-type copies of *acs-1* that rescued the larval lethality. Some of the progeny of *acs-1(gk3066);Ex[acs-1(full)]* animals, but not all, did display the Emb phenotype observed in *acs-1(RNAi)*^{C17ISO} animals (Fig. 1D). We hypothesized that the Emb phenotype in the *acs-1(gk3066);Ex[acs-1(full)]* animals resulted from a loss of *acs-1* expression in one or more tissues in parental worms with mosaic distribution of the extra chromosomal array.

Notably, analysis using either RNAi or the genetic mutation showed that the Emb phenotype was associated with the presence of C17ISO, supplied exogenously in *acs-1(RNAi)*^{C17ISO} or synthesized endogenously in *acs-1(gk3066);Ex[acs-1(full)]* animals (see below). These data suggested that in addition to the role in C17ISO biosynthesis, ACS-1 also promotes embryogenesis by regulating C17ISO metabolism.

Expression of acs-1 in the somatic gonad is necessary and sufficient for embryogenesis

To identify the tissue where *acs-1* expression is essential for embryogenesis, we first examined wild-type expression of the gene by using an integrated transgene of *acs-1(full)::GFP* (a full-length ACS-1::GFP fusion protein driven by the *acs-1* promoter) and in situ hybridization. In addition to the neuronal and intestinal expression previously detected using an *acs-1* promoter-driven GFP expression construct (Kniazeva et al. 2004), we observed prominent GFP fluorescence in the somatic gonad of adults but not in that of larvae (Fig. 2A,B; Supplemental

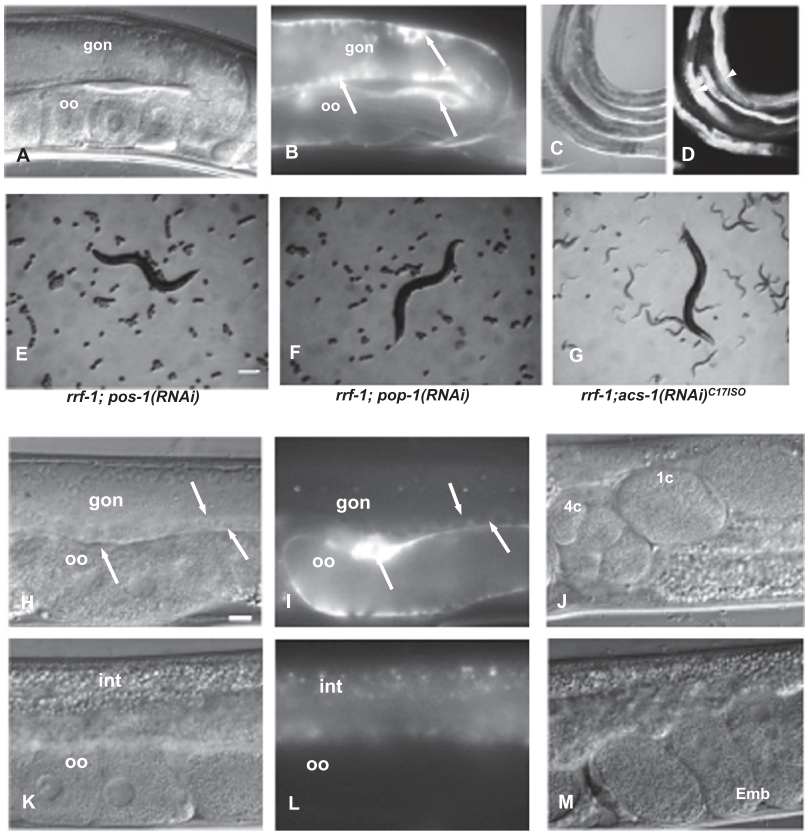

Figure 2. *acs-1* expression in the somatic gonad, but not in the germline or the intestine, is critical for embryogenesis. (*A*,*B*) DIC and corresponding fluorescence images showing the adult mid-body expressing an integrated and functional *acs-1(full)::GFP* reporter. (gon) Distal part of the gonad arm; (oo) oocytes in the proximal part of the gonad arm. Arrows in *B* point to fluorescence at the outer edge of the gonad tube corresponding to somatic gonad sheath cells. Bar, 15 μm. (*C*,*D*) DIC and corresponding fluorescent images illustrating the rescue of *acs-1(gk3066)* mutants to growth with an extra chromosomal array (*C*); all rescued animals expressed the *acs-1(full)::GFP* fusion gene in the intestinal, whereas the expression of CAN neurons was nonessential (*D*), as indicated by arrowheads ($n > 500$). (*E–G*) Microscopic images of RNAi-treated worms showing that *acs-1* expression in germline, if any, is irrelevant to its role in embryogenesis. An *rrf-1(lf)* mutant resistant to somatic but not germline RNAi was used in the experiment. Feeding with control RNAi strains (*pos-1* and *pop-1*) resulted in robust embryonic arrest (100%, $n > 200$), confirming the effectiveness of RNAi in the germline in this strain. A similar result for *par-1(RNAi)* is not shown. *acs-1(RNAi)*^{C17ISO} treatment of the *rrf-1(lf)* mutant did not cause Emb. Bar, 200 μm. (*H–M*) DIC and fluorescence images illustrating a tight correlation between the absence of somatic gonad expression of the *acs-1(full)::GFP* transgene in *acs-1(gk3066)* mutant worms and the Emb phenotype. The images of the gonads in *H–J* and *K–M* were obtained from the same adult animal. All (100%) GFP-positive gonads ($n = 156$) (*H*) produced wild-type embryos (*J*). Arrows in *H* and *I* point to fluorescence in the somatic gonad. In *J*, 1c and 4c mark a one-cell and a four-cell embryo, respectively. All (100%) GFP-negative gonads ($n = 68$) (*L*) produced embryos with the Emb phenotype (*M*). (Int) Intestine. Bar, 15 μm.

Fig. S2A–L,S,T). Results from RNA in situ hybridization confirmed *acs-1* expression in the somatic gonad, while no expression was detected in the germline (Supplemental Fig. S2M–R).

Since transgenic GFP expression may be silent in the germline, and RNA in situ hybridization may not be sensitive enough to detect very low levels of *acs-1* germline expression, we performed germline-specific RNAi analysis to determine whether there was a requirement for *acs-1* germline expression. We treated *rrf-1(pk1417)*, which is resistant to somatic RNAi but sensitive to germline RNAi (Sijen et al. 2001), with *acs-1(RNAi)*^{C17ISO}. *pop-1(RNAi)*, *pos-1(RNAi)*, and *par-1(RNAi)* were used as positive controls for germline-specific RNAi (Sijen et al. 2001). We found that *rrf-1* animals fed control RNAi laid 100% dead eggs, indicating that RNAi was highly effective in the germline of this strain (Fig. 2E,F). In contrast, *rrf-1;acs-1(RNAi)*^{C17ISO} animals developed normally for at least three generations (Fig. 2G). These results indicated that expression of *acs-1* in the germline, if any, was not essential for embryogenesis and that its expression in somatic cells was necessary and sufficient for this function.

To investigate the requirement for *acs-1* in specific somatic tissues with regard to its embryonic function, we created an *acs-1(gk3066);Ex[acs-1(full)::GFP]* strain in which the ACS-1(full)::GFP protein rescued larval lethality associated with the deletion mutation to an extent similar to that of the *acs-1(gk3066);Ex[acs-1(full)]* strain. Microscopic evaluation of *acs-1(gk3066);Ex[acs-1(full)::GFP]* adults revealed a prominent GFP fluorescence in the intestinal cells of all rescued animals ($n > 500$), whereas CAN neuron expression was only apparent in some (Fig. 2C,D). This indicated that the expression of *acs-1* in the gut was necessary to overcome larval lethality. GC analysis confirmed that rescued animals regained the ability to synthesize C17ISO (data not shown).

Remarkably, somatic gonad expression of the *acs-1(full)::GFP* transgene was tightly correlated with the occurrence of> wild-type embryos; 100% of the gonads positive for GFP ($n = 156$) produced wild-type embryos, and 100% of the GFP-negative gonads ($n = 68$) produced dead eggs (Fig. 2H–M). Moreover, the expression of *acs-1(full)::GFP* in only one of the two gonads did not rescue the Emb phenotype in the other (Fig. 2H–M). These observations indicated that ACS-1 functions locally in the somatic gonad to influence embryonic development.

Results of additional experiments reinforced the above conclusion. Briefly, when *acs-1* expression was disrupted

in the intestine (but not in the somatic gonad) in the presence of dietary C17ISO, it did not result in Emb (Supplemental Fig. S2W–ac; Supplemental Material). In contrast, when *acs-1* expression was inhibited in the somatic gonad by somatic gonad-specific RNAi, the remaining expression of *acs-1* in the intestine, neurons, and possibly other tissues was insufficient to prevent the Emb phenotype (Materials and Methods; Supplemental Fig. S2ad–ag).

Together, these results indicate that (1) C17ISO, both supplied exogenously and synthesized endogenously, can become "toxic" to the embryo in the absence of *acs-1*; (2) the somatic gonad is the tissue where expression of *acs-1* eliminates this "toxicity"; and (3) ACS-1 functions in a local intercellular pathway between the somatic gonad and the germline (as indicated by the fact that the somatic gonad arm expressing *acs-1* can only protect embryos developing from its associated germline).

ACS-1–C17ISO interaction ensures proper membrane dynamics in early embryos

Prominent cellular events in the wild-type zygote include formation of the perivitelline space and vigorous movement of plasma membrane during ruffling, pseudocleavage, and furrowing (Fig. 3A–E). Strikingly, none of these post-fertilization hallmarks were observed in either *acs-1(RNAi)*^{C17ISO} or embryos from *acs-1(gk3066);Ex[acs-1(full)::GFP]* animals that lost *acs-1* expression in the somatic gonad. Instead, the cytoplasm of these embryos appeared to occupy the entire egg (i.e., egg-filling phenotype) without any sign of wild-type membrane dynamics (Fig. 3F–I). This phenotype did not represent a quiescent state because the cell cycle proceeded at a nearly normal rate, but the separation of divided nuclei failed at the first or subsequent cell divisions. Since *acs-1(RNAi)*^{C17ISO} Emb mimicked that of embryos from *acs-1(gk3066);*

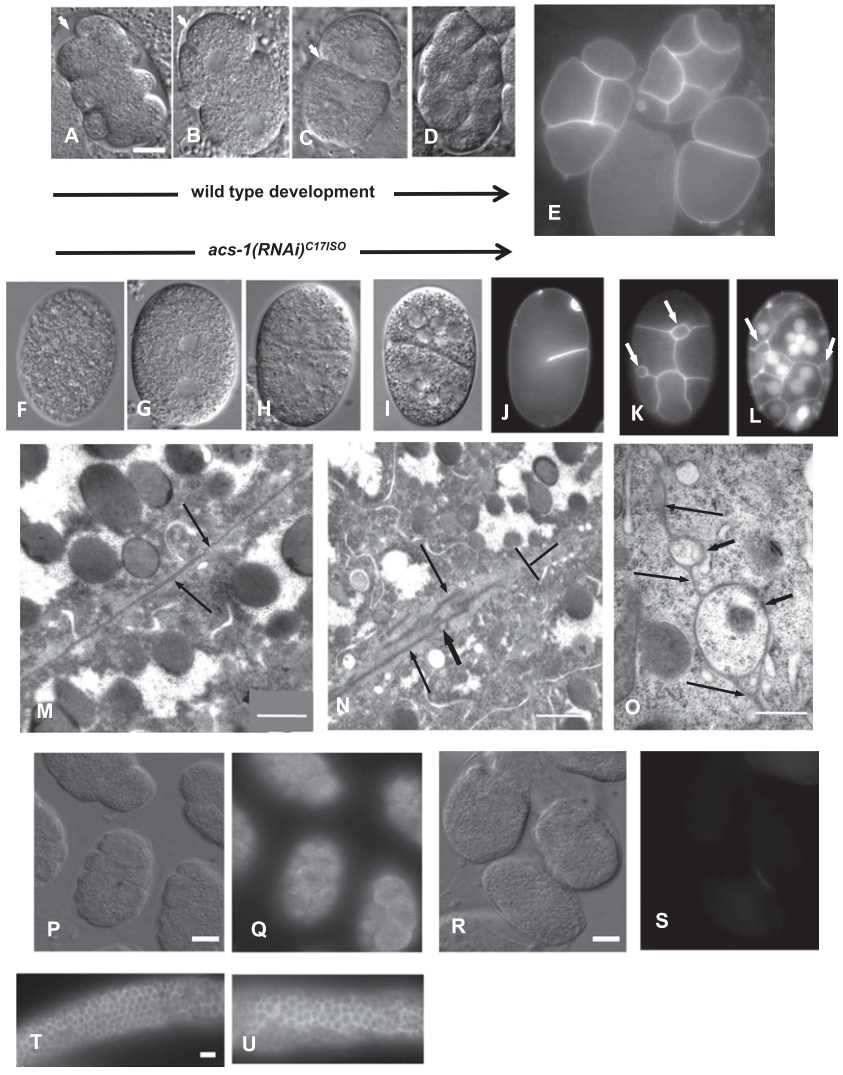

Figure 3. Formation of the perivitelline space, normal membrane biogenesis and dynamics, and exocytosis of GAGs are disrupted in *acs-1(RNAi)*^{C17ISO} embryos. (*A–L*) DIC and fluorescent images of wild-type (*A–E*) and *acs-1(RNAi)*^{C17ISO} (*F–K*) embryos at matching developmental stages. (*A–D*) Wild-type embryos form the perivitelline space (arrowheads) and undergo vigorous membrane remodeling during ruffling (*A*), pseudocleavage (*B*), and first cytokinesis (*C*) that are clearly visible. (*E*) Wild-type plasma membrane contours in one-cell to six-cell embryos are highlighted with the $PH_{PLC1\partial1}$::GFP reporter. (*F–I*) *acs-1(RNAi)*^{C17ISO} embryos shown at the same stages corresponding to those in *A–D* fail to form the perivitelline space and lack any visible membrane activity. (*I*) Cell divisions do not properly follow nuclei divisions. See also Supplemental Figure S3. (*J–L*) Plasma membrane fails to elongate after the first (*J*) or subsequent (*K,L*) cell cycles and forms unusual membranous structures (arrows). Nuclei in *L* are highlighted with DAPI stain. (*M–O*) Electron micrographs show the cell membrane of dividing wild-type (*M*) and *acs-1(RNAi)*^{C17ISO} (*N,O*) blastomeres. (*M*) Cell membranes after completion of cytokinesis look like a single straight line in this section. (*N,O*) In contrast to *M*, interrupted, branched plasma membranes with unusual membranous structures are observed in *acs-1(RNAi)*^{C17ISO} embryos. Black arrows point to the membrane from the sides of two fully (*M*) or partially (*N,O*) separated blastomeres. Short arrows indicate unusual membranous formations, and the T-bar in *N* shows a discontinuance of a dividing membrane. (*P–S*) DIC and fluorescence images of wild-type (*P,Q*) and *acs-1(RNAi)*^{C17ISO} (*R,S*) embryos stained with an anti-chondroitin sulfate antibody (Ab). All images capture the surface of the embryos, illustrating that chondroitin sulfate is delivered to the perivitelline space in wild-type but not *acs-1(RNAi)*^{C17ISO} embryos (cf. *Q* and *S*). (*T,U*) The distribution of chondroitin sulfate in the gonad appears to be similar in wild type (*T*) and *acs-1(RNAi)*^{C17ISO} (*U*), indicating that the synthesis of this GAG is not disrupted. Bars, 15 μm.

Ex[acs-1(full)::GFP] animals that lost *acs-1* expression in the somatic gonad, we carried out further detailed phenotypic analysis using RNAi that is more technically efficient.

Using a $PH_{PLC1\partial1}$::GFP reporter (PH, pleckstrin homology domain from phospholipase C that binds to phosphatidylinositol lipids in plasma membranes) (Hurley and Meyer 2001; Audhya et al. 2005), we showed that the cell cleavage could be initiated in some embryos despite the complete absence of ruffling and pseudocleavage, but proper elongation of the dividing membrane often ceased (Fig. 3J; Supplemental Fig. S3A–C). In other embryos, cellular cleavage reached completion but enclosed more than one nucleus within a single daughter cell (Fig. 3I,K,L). As a result, these embryos displayed the Emb phenotype with characteristic formation of multinucleated cells and accumulation of peculiar membranous structures in the cytoplasm (Figs. 3I–L, 4F).

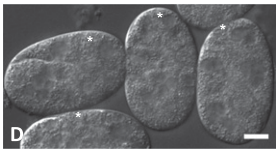

E

[C17ISO] in supplement	% Emb (Emb/total)
0.00 mM	0.0 (0>200)
0.17 mM	7.8 (4/51)
0.34 mM	32 (22/68)
0.50 mM	90.4 (104/115)
1.00 mM	98.1 (102/104)

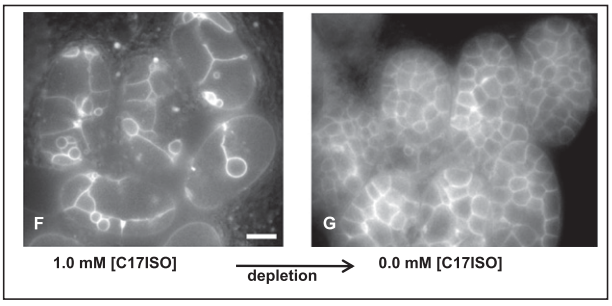

Figure 4. Penetrance of the Emb phenotype correlates with the C17ISO concentration fed to *acs-1(RNAi)*^{C17ISO} adults. (*A–D*) DIC images showing representative embryos isolated from adults grown on *acs-1(RNAi)* plates supplemented with C17ISO at the indicated concentrations. Stars in *C* and *D* indicate the embryos with the Emb phenotype. (*E*) Results indicating that the increase in the concentration of C17ISO supplement is accompanied by an increase in the percentage of dead embryos. (*F,G*) Fluorescence images showing that depletion of C17ISO correlates with decreased instances of abnormal membranous structures and increased cases of wild-type cell division. The embryos were released from adults fed with 1 mM C17ISO (*F*) and from adults that were transferred at the L4 stage from plates supplemented with 1 mM C17ISO to plates without supplementation (*G*). See also Supplemental Table S1 for numerical values. The membrane is highlighted with a $PH_{PLC1\partial1}$::GFP reporter. Bars, 15 μm.

Electron microscopy (EM) analysis of dividing blastomeres in *acs-1(RNAi)*^{C17ISO} embryos confirmed instances of unusual membrane formation, revealing membrane branching, multiple breaks, and the presence of various membranous shapes alongside the cleavage furrow (Fig. 3M–O). These data indicated that membrane biogenesis took place in *acs-1(RNAi)*^{C17ISO} zygotes but that it was severely disordered. This phenotype has not been previously reported in any *C. elegans* mutant. This finding demonstrated that the ACS-1–C17ISO interaction critically impacts membrane properties important for membrane-related cellular events during early embryogenesis.

acs-1(RNAi)^{C17ISO} *embryos do not display obvious defects in eggshell structure, osmotic sensitivity, or anterior–posterior (A–P) polarity*

The egg-filling phenotype and the failure to undergo ruffling, pseudocleavage, and cytokinesis are known characteristics of a number of mutants defective in the formation of the extracellular matrix (ECM), which constitutes the eggshell and perivitelline space (Tagawa et al. 2001; Hwang et al. 2003; Mizuguchi et al. 2003; Rappleye et al. 2003; Wang et al. 2005; Olson et al. 2006; Sato et al. 2008). It has also been shown that actomyosin contractility is essential for membrane remodeling during ruffling, pseudocleavage, and cytokinesis (Gönczy and Rose 2005; Maddox et al. 2005, 2007).We thus analyzed the eggshell structure and tested cellular processes, such as osmotic sensitivity and establishment of A–P polarity. We did not obtain any evidence that would indicate that a defect in these processes causes the *acs-1(RNAi)*^{C17ISO} embryonic phenotype (Supplemental Fig. S3; Supplemental Material).

Exocytosis of glycosaminoglycans (GAGs) essential for ECM formation is defective in acs-1(RNAi)^{C17ISO} *embryos*

Work by several laboratories has shown that GAGs and proteoglycans, delivered by exocytosis to the ECM shortly after fertilization, are essential for the generation of the perivitelline space and cytokinesis (Hwang and Horvitz 2002; Hwang et al. 2003; Mizuguchi et al. 2003; Wang et al. 2005; Olson et al. 2006; Sato et al. 2008). Since one of the prominent features of *acs-1(RNAi)*^{C17ISO} embryos is an absence of a visible perivitelline space, we examined the possibility that exocytosis was impaired in *acs-1(RNAi)*^{C17ISO} embryos.

An anti-chondroitin sulfate antibody has been previously used to detect the presence of chondroitin (one of the secreted GAGs) on the cell surface of embryonic cells and gonad (Mizuguchi et al. 2003). Using this antibody, we observed the reported staining for wild-type embryos (Fig. 3P,Q) but did not detect the antigen on the *acs-1(RNAi)*^{C17ISO} embryo cell surface (Fig. 3R,S). Biosynthesis of chondroitin was not disrupted in the *acs-1(RNAi)*^{C17ISO} animals, as it was readily detectable in the gonads (Fig. 3T,U).

These data suggested that the absence of the perivitelline space in *acs-1(RNAi)*^{C17ISO} embryos may have been caused, at least in part, by defective exocytosis of GAGs.

However, other features of the *acs-1(RNAi)*^{C17ISO} Emb phenotype could not be explained solely by failed delivery of GAGs. For example, the prominent accumulation of abnormal membranous structures in *acs-1(RNAi)*^{C17ISO} embryos was not observed in *sqv* mutants defective in GAG biosynthesis (Hwang and Horvitz 2002; Hwang et al. 2003; Mizuguchi et al. 2003; Wang et al. 2005; Olson et al. 2006; Sato et al. 2008; data not shown). In addition, there was a significant difference in the dynamics of attempted cleavage between the *sqv* mutants and *acs-1(RNAi)*^{C17ISO} embryos; while the cleavage furrow retracted after initiation in the *sqv* embryos, the cleavage furrow failed to elongate properly but did not retract in *acs-1(RNAi)*^{C17ISO} embryos ($n > 300$) (Supplemental Fig. S3A–C).

Moreover, the failure of cleavage in *acs-1(RNAi)*^{C17ISO} embryos did not always occur during the very first cell division, and cleavage failure in subsequent cell divisions was always accompanied by erratic membrane formations (Figs. 3K,L,N,O, 4F). These differences suggested that the alterations in membrane properties in *acs-1(RNAi)*^{C17ISO} embryos affected more than just exocytosis of GAGs.

The acs-1(RNAi)^{C17ISO} *affects plasma membrane behavior without globally disrupting formation of endocytic and exocytic vesicles*

It is conceivable that some vesicle compartments involved in ECM formation and cytokinesis might be altered in *acs-1(RNAi)*^{C17ISO} embryos. To examine subcellular compartments that might be affected in *acs-1(RNAi)*^{C17ISO} embryos, we analyzed several fluorescence-labeled reporters specific for endocytic and exocytic vesicles. However, no differences were detected between wild-type and *acs-1(RNAi)*^{C17ISO} embryos in the localization of caveolin-enriched (CAV-1::GFP reporter) or RAB-11::GFP-labeled secretary cortical granules or in their plasma membrane receptor (SYN-4::GFP reporter) (Sato et al. 2006, 2008) with regard to the vesicles' distribution and morphology. Similarly, no difference was observed in the distribution and morphology of RAB-5::GFP-positive endocytic compartments (Sato et al. 2005) or in the endoplasmic reticulum (ER) structures (SP12::GFP reporter highlighting an ER resident protein, signal peptidase SP12) (Rolls et al. 2002; Poteryaev et al. 2005). Therefore, the defects in *acs-1(RNAi)*^{C17ISO} embryos appeared to be restricted to the plasma membrane as described above.

Penetrance of the Emb phenotype in acs-1(RNAi)^{C17ISO} *animals correlates with C17ISO concentration, but not with C17ISO-independent changes in lipid composition*

As mentioned above, *acs-1(RNAi)* and acs-1(gk3066); Ex[acs-1(full)::GFP] animals reach adulthood only in the presence of C17ISO that is supplied exogenously or synthesized endogenously, respectively. To investigate the effect of C17ISO on embryonic lethality, we examined the phenotypes of acs-1(RNAi)C17ISO animals growing in the presence of different C17ISO concentrations. Wild-type worms were treated with *acs-1(RNAi)* from the time of hatching on plates supplemented with 0.0 mM, 0.17 mM, 0.34 mM, 0.5 mM, or 1.0 mM C17ISO. We observed at low concentrations (0.17 mM and 0.34 mM) that only a small number of animals reached adulthood, but these rescued adults produced wild-type embryos. At higher concentrations, the effect was reversed; more animals developed to wild-type adults, but these rescued adults produced fewer or no wild-type embryos (Fig. 4A–E).

Using a PHPLC1∂1::GFP reporter, we tested the effect of C17ISO depletion on plasma membrane dynamics. *acs-1(RNAi)* C17ISO young adults were transferred to *acs-1(RNAi)* plates without supplement to deplete the next generation of C17ISO. We found that a decrease in accumulated C17ISO (confirmed by GC analysis of the FA composition in eggs) (data not shown) was associated with a prominent increase in the instances of successful cell divisions and decreased vesiculation (Fig. 4F,G; Supplemental Table S1). These results indicated that the presence of C17ISO or its metabolite correlated with the Emb phenotype in *acs-1(RNAi)*-treated animals.

We did not observe the specific Emb phenotype associated with *acs-1(RNAi)*^{C17ISO} in animals treated with RNAi targeting several other FA- and energy metabolism-related genes, even though prominent changes in lipid composition and embryonic lethality were observed in many of these animals (Supplemental Fig. S4A–I; Supplemental Material).

Distinctive changes in phospholipid composition correlating with the Emb phenotype are present in lipid extracts from acs-1(RNAi)^{C17ISO} *embryos*

The findings that C17ISO affects embryonic development and does so only in the absence of *acs-1* expression in the somatic gonad suggested that ACS-1 may act on C17ISO by directing its incorporation into particular lipids. To test this hypothesis, we compared lipid extracts isolated from wild-type and *acs-1(RNAi)*^{C17ISO} embryos using mass spectrometry (MS) analysis. We specifically screened for changes in the lipid composition that correlated with the penetrance of the Emb phenotype by analyzing samples isolated from *acs-1(RNAi)*^{C17ISO} embryos that had developed in adults fed with 1 mM or 0.1 mM C17ISO. Total ion chromatograms indicated a glycerophospholipid (PL) fraction that was consistently greater in *acs-1(RNAi)*$^{1.0\ mM\ C17ISO}$ than in *acs-1(RNAi)*$^{0.1\ mM\ C17ISO}$ or untreated wild-type samples (Fig. 5A). MS spectra resolved individual peaks in a range of 680–760 m/z in this fraction (Supplemental Fig. S4J). Tandem electrospray ionization (ESI)-MS spectra of PLs within this mass range obtained by precursor scan of 269.2 in negative mode (loss of C17ISO ion scan) confirmed that these lipids contained C17ISO (Fig. 5B).

Strikingly, the major peaks in the *acs-1(RNAi)*$^{1.0\ mM\ C17ISO}$ samples differed from those in untreated wild-type samples by 4 m/z (Fig. 5B). These shifts could have resulted from structural differences in either fatty acyl chains or the phosphate head group attached to a glycerol backbone

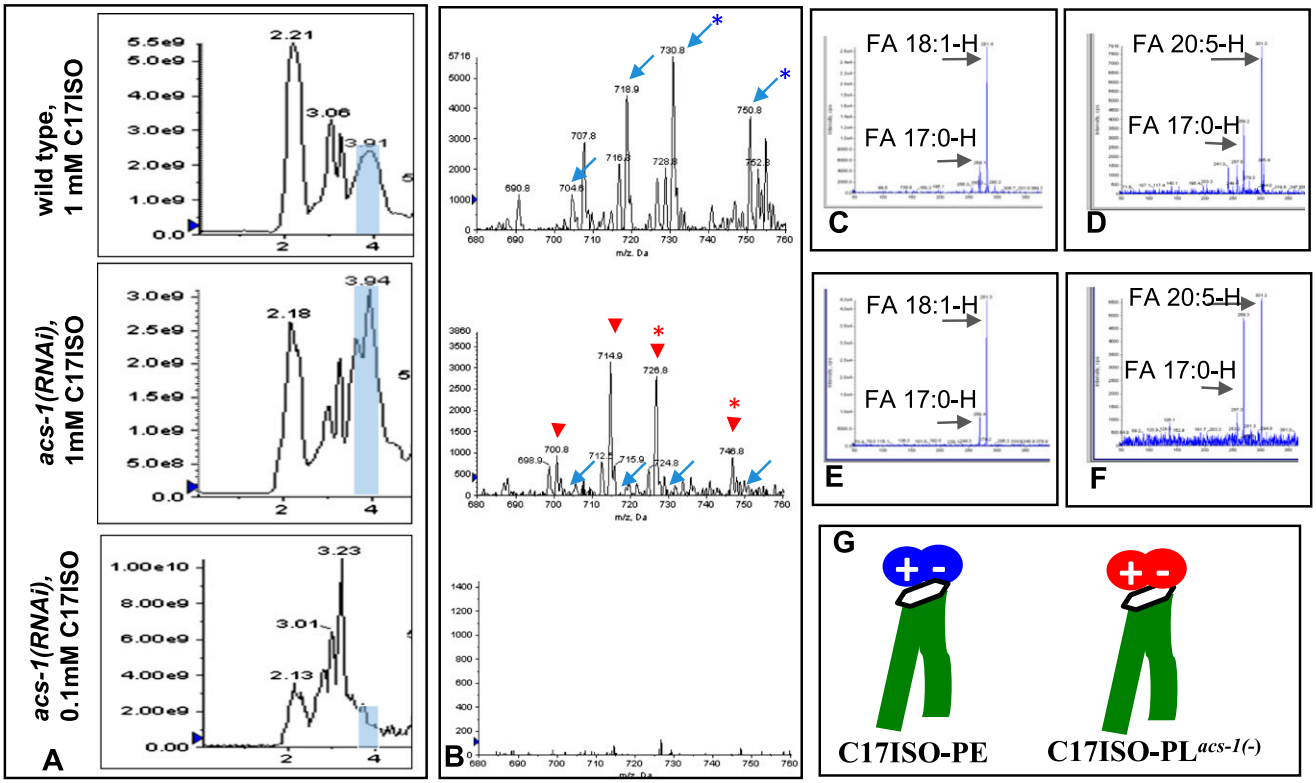

Figure 5. Distinctive changes in phospholipid composition in lipid extracts from *acs-1(RNAi)*^{C17ISO} embryos correlate with the Emb phenotype. (*A–F*) MS analysis of a group of C17ISO-containing PLs in the embryos associated with the Emb phenotype. The data are representative of three consistent biological replicates. Part of the data is presented in Supplemental Figure S4J. (*A*) Total ion chromatograms of lipid extracts from the indicated embryonic samples show lipid fractions with retention times from 0 to 5 min. Shaded areas indicate the lipid fraction that is increased in lipid extracts from *acs-1(RNAi)*$^{1\ mM\ C17ISO}$ but not in that from wild-type or C17ISO-deficient *acs-1(RNAi)*$^{0.1\ mM\ C17ISO}$ embryos. Following ESI-MS, analysis resolved several individual peaks within the fraction in the range of 650–800 *m/z* (Supplemental Fig. S4J). (*B*) Tandem ESI-MS spectra of C17ISO-containing lipids obtained by precursor scanning of 269.2 in negative mode (loss of C17ISO ion scan). Only the spectra within the mass range of 680–760 *m/z* are shown. The C17ISO-containing PE species (marked with arrows) are the major components in wild-type (*top* panel) but not in *acs-1(RNAi)* (*middle* and *bottom* panels) samples, indicating that their synthesis is ACS-1-dependent. Major peaks in *acs-1(RNAi)*$^{1\ mM\ C17ISO}$ samples differ from those in wild type by 4 *m/z* (arrowheads). These compounds do not require ACS-1 for their synthesis and are only minor constituents in the wild-type fraction. These metabolites are not detectable in extracts from C17ISO-deficient [*acs-1(RNAi)*$^{0.1\ mM\ C17ISO}$] embryos (*bottom* panel) or in lipids from adult worms (not shown). (*C*,*D*) Tandem mass spectra of two PE peaks ([730.6(-H)$^-$] and [750.6(-H)$^-$], shown in the *top* panel of *B*, marked with arrows and stars). (*E*,*F*) Tandem mass spectra of the two peaks of unknown lipids ([726.6(-H)$^-$] and [746.6(-H)$^-$], shown in the *middle* panel of *B*, marked by arrowheads and stars). The acyl chains in the unknown lipids (*E*,*F*) are the same as those in PEs (*C*,*D*), respectively. (*G*) Cartoon illustrating the differences in C17ISO-containing phospholipids analyzed in *C–F*. While the two structures have identical acyl chain composition (green tails) and glycerol backbone (black ring), they differ in the polar head group (blue and red subjects). We refer to them as C17ISO-PE (ACS-1-dependent) and C17ISO-PL$^{acs-1(-)}$ (ACS-1-independent).

in PLs. Subsequent tandem MS and normal phase liquid chromatography (NPLC-MS) analyses revealed that the major PL in the wild-type and *acs-1(RNAi)*$^{1\ mM\ C17ISO}$ samples contained the same combination of acyl chains. For example, PL^{WT} [730.6(-H)$^-$] and PL$^{acs-1(-)C17ISO}$ [726.6(-H)$^-$] were both composed of C17ISO and C18:1, whereas PL^{WT} [750.6(-H)$^-$] and PL$^{acs-1(-)C17ISO}$ [746.6(-H)$^-$] contained C17ISO and C20:5 (Fig. 5C–F). In the wild-type sample, the head group of the major C17ISO-containing PL was identified as ethanolamine (data not shown), and therefore these lipids were phosphatidylethanolamine (PE) species (termed C17ISO-PE). The identity of the head group of the major C17ISO-containing PL species in *acs-1(−)*$^{1.0\ mM\ C17ISO}$ [termed C17ISO-PL$^{acs-1(-)}$] remains to be determined (Fig. 5G).

The difference in the levels of C17ISO-PE and C17ISO-PL$^{acs-1(-)}$ between wild-type and *acs-1(−)*^{C17ISO} embryos indicated that C17ISO-PE biosynthesis required ACS-1 function, while the synthesis of C17ISO-PL$^{acs-1(-)}$ did not. The synthesis of C17ISO-PL$^{acs-1(-)}$ thus depends on other ACS enzymes. Therefore, in wild-type worms, ACS-1 may compete with other ACSs for the C17ISO substrate to produce C17ISO-PE, and possibly other C17ISO-containing lipids, and indirectly decrease the relative levels of C17ISO-PL$^{acs-1(-)}$ that are present at minute levels in wild-type samples (Fig. 5B, top and middle panels). Since a decrease of both C17ISO-PE and C17ISO-PL$^{acs-1(-)}$ species did not cause Emb in *acs-1(RNAi)*$^{0.1\ mM\ C17ISO}$ animals (Fig. 5B), the dominant presence of C17ISO-PL$^{acs-1(-)}$ is likely necessary for the manifestation of the embryonic phenotype.

While the exact structure of C17ISO-PL$^{acs\text{-}1(-)}$ is being currently investigated, the current data clearly indicated that ACS-1 and C17ISO affected a specific aspect of PL composition that may play important roles in early embryogenesis. Importantly, no significant differences in lipid profiles were detected between the lipid extracts obtained from wild-type or *acs-1(RNAi)*$^{1.0\ mM\ C17ISO}$ adults, and no changes in the levels of C17ISO-containing triacylglycerols (i.e., triacylglycerols or TAGs, fats) were observed between the embryonic samples (Supplemental Fig. S4K).

The embryonic phenotype of acs-1(RNAi)^{C17ISO} is suppressed by mutations causing hyperactive IP_3 signaling

Exocytosis of the embryonic ECM has been shown to depend on IP_3-regulated calcium signaling in many organisms (Becchetti and Whitaker 1997; Chang et al. 1999; Stricker 1999; Abbott and Ducibella 2001; Webb et al. 2008). Although a link between the IP_3 pathway and embryonic exocytosis has not been thoroughly investigated in *C. elegans*, an observation of egg-filling multinucleated embryos resembling *acs-1(RNAi)^{C17ISO}* embryos was reported in mutants with decreased IP_3 signaling (Walker et al. 2002). In addition, disrupting the function of RAB-11 GTPase (a major regulator of Ca^{2+}-induced exocytosis located on the membrane of excretory vesicles) or SYN-4 (calcium-sensing target SNARE located on plasma membranes) was shown to mimic the blockage of chondroitin biosynthesis that also results in the egg-filling phenotype, failed cytokinesis, and multinucleated blastomeres (Jantsch-Plunger and Glotzer 1999; Sato et al. 2008). As reported above, we observed that the expression and subcellular localization of RAB-11 and SYN-4 in *acs-1(RNAi)^{C17ISO}* embryos were not different from wild type.

We then investigated whether a potential failure of IP_3 signaling could cause the *acs-1(RNAi)^{C17ISO}* Emb phenotype. If IP_3 production at the plasma membrane in *acs-1(RNAi)^{C17ISO}* embryos is reduced, then raising the level of IP_3 or enhancing the sensitivity of the IP_3 receptor may rescue the Emb phenotype. To test this hypothesis, we carried out a genetic analysis using a loss-of-function (*lf*) mutation in *ipp-5* (encoding a type I phosphatase that converts IP_3 to inositol 1,4 bisphosphate [IP_2]) and a gain-of-function (*gf*) mutation in the only IP_3 receptor gene, *itr-1* (Clandinin et al. 1998; Baylis et al. 1999; Dal Santo et al. 1999; Bui and Sternberg 2002). Specifically, mutants and wild-type controls were treated with *acs-1(RNAi)* in the presence or absence of C17ISO supplementation (Supplemental Fig. S5). We found that Emb was suppressed in both mutants with hyperactive IP_3 signaling (Fig. 6A).

Microscopic evaluation revealed that the rescue effect of the *ipp-5* mutation on the Emb phenotype in *acs-1(RNAi)^{C17ISO}* was, in fact, much stronger than that indicated by the number of hatched progeny per adult shown in Figure 6A. The *ipp-5(lf)* mutation alone frequently produced dead embryos with phenotypes distinctly different from the phenotype of *acs-1(RNAi)^{C17ISO}* embryos (Fig. 6B,C). The majority of the embryos in the uterus of *ipp-5(lf);acs-1(RNAi)^{C17ISO}* animals were similar in appearance to those of *ipp-5(lf)* and did not have defects in perivitelline space formation or in cytokinesis during early embryogenesis [characteristics specific to *acs-1(RNAi)^{C17ISO}*] (Fig. 6B,D). These data indicated that elevating IP_3 signaling was sufficient to suppress the *acs-1(RNAi)^{C17ISO}*-caused embryonic lethality.

RNAi silencing of the *itr-1* gene resulted in suppression of IP_3 signaling and caused sterility (Ste) in the first generation (Kamath et al. 2003; Green et al. 2011). Using the $PH_{PLC1\partial1}$::GFP reporter to examine *itr-1(RNAi)* animals, we found that peculiar vesiculation of plasma membrane in the proximal gonad blocked the contact between oocytes and spermatheca (Fig. 6G,H). In rare cases when *itr-1(RNAi)* embryos were nevertheless produced (1%, n = 200), they were phenotypically indistinguishable from *acs-1(RNAi)^{C17ISO}* embryos (Fig. 6I). The unique and marked similarity between aberrant plasma membrane formations in the *itr-1(RNAi)* gonads and embryos (Fig. 6G–I) suggests a common mechanism involving the IP_3 pathway in regulating plasma membrane dynamics and supports the idea that the impairment in IP_3 signaling may mediate the effect of *acs-1(RNAi)^{C17ISO}* on membrane dynamics in the zygote.

Discussion

In this study, we combined genetics with biochemical analysis to investigate a connection between the ACS-1-mediated metabolism of C17ISO and embryonic development in *C. elegans*. C17ISO is present in many organisms, including humans, but its function is unknown. We showed that the expression of *acs-1* in the somatic gonad guides the incorporation of C17ISO into certain phospholipids and consequently critically affects the composition of C17ISO-containing phospholipids in the zygote. We also provide evidence for a model in which C17ISO-lipid composition promotes IP_3 signaling that in turn regulates membrane dynamics in the early embryo (Fig. 7).

More generally, this work provides novel insight into the mechanism by which ACS enzymes regulate specific physiological functions by directing specific FAs to specific lipid species at specific locations.

Tissue specificity of ACS-1 functions

Like most of the annotated *acs* genes in *C. elegans*, *acs-1* has a broad expression pattern that partially overlaps with other *acs* genes (*acs-2*, *acs-3*, *acs-4*, *acs-5*, *acs-11*, *acs-13*, *acs-19*, *acs-20*, and *acs-22*) (http://www.wormbase.org). However, the role of *acs-1* in C17ISO metabolism and its physiological outcome uncovered in this study is not redundant. We used multiple approaches to demonstrate that the expression of *acs-1* in the somatic gonad is necessary and sufficient for embryogenesis (Fig. 2; Supplemental Fig. S2M–ag). This conclusion is consistent with a model in which the protective function of ACS-1 comes from somatic cells that are physically close to the gonad. This model is also supported by the finding that ACS-1-associated changes in the composition of C17ISO-

A Strains	Hatched progeny/ 100 adults	# of adults examined
acs-1(RNAi)^{C17ISO}	1.8	392
ipp-5(sy605 lf); acs-1(RNAi)^{C17ISO}	950	79
itr-1(sy290 gf); acs-1(RNAi)^{C17ISO}	126.9	55
itr-1(sy331 gf); acs-1(RNAi)^{C17ISO}	310	60
itr-1(sa73 lf); acs-1(RNAi)^{C17ISO}	0.0	>300

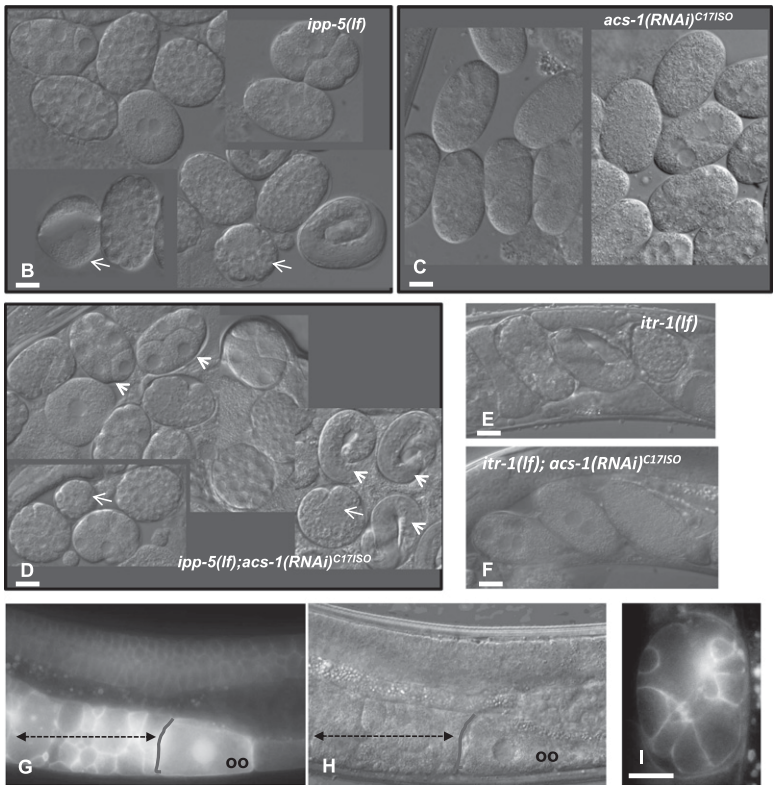

Figure 6. Hyperactivity in IP_3 signaling suppresses the specific embryonic defects caused by *acs-1(RNAi)^{C17ISO}*, whereas inhibiting IP_3 signaling causes phenotypes resembling that of *acs-1(RNAi)^{C17ISO}*. (*A*) Summary data showing that *ipp-5(lf)* and *itr-1(gf)* mutations partially rescue the embryonic lethality caused by *acs-1(RNAi)^{C17ISO}* treatment. Hatched progeny of animals maintained on corresponding plates were counted 3 d after egg laying had begun. The actual extent of rescue of the *acs-1(RNAi)^{C17ISO}*-associated Emb phenotype is significantly higher than that indicated by the numbers, considering that mutations in *ipp-5(lf)* and *itr-1(gf)* cause partial Emb on their own, although it is distinctively different from the Emb phenotype of *acs-1(RNAi)^{C17ISO}* (see *B*,*C*). (*B–F*) DIC images of embryos at different developmental stages dissected from gravid adults of the indicated genotype and/or treatment. The *ipp-5(sy605 lf)* mutation, known to enhance IP_3 signaling, causes a partial and variable late Emb phenotype (*B*; examples are indicated by arrows), which is different from the Emb caused by *acs-1(RNAi)^{C17ISO}* treatment as shown in *C* (see also Fig. 3F–I). (*D*) In the *ipp-5(sy605);acs-1(RNAi)^{C17ISO}* animals, the *acs-1(RNAi)^{C17ISO}*-associated Emb phenotype characterized by egg-filling embryos with multinuclear cells is strongly suppressed [arrowheads point to some examples of suppressed embryos, and arrows point to examples of embryos with the *ipp-5(sy605lf)* late stage Emb phenotype]. (*E*,*F*) The *itr-1(sa73 lf)* mutation that reduces IP_3 signaling does not rescue the early embryonic defects in *acs-1(RNAi)^{C17ISO}* worms. Bars, 15 μm. (*G*,*H*) Fluorescent and DIC images illustrating the sterile phenotype of *itr-1(RNAi)* gonads characterized by profound vesiculation in the proximal end (dotted two-headed arrow; [oo] oocyte). The tissue indicated by the arrow is DAPI-negative (not shown) and thus does not contain nuclei or present ectopic germline proliferation. (*I*) Fluorescent image of Emb of rarely produced *itr-1(RNAi)* embryos (1%, n = 200), similar to that observed in *acs-1(RNAi)^{C17ISO}* (cf. Fig. 4F).

containing phospholipids in *acs-1(RNAi)^{C17ISO}* embryos were not detected in adults. We propose that activation of C17ISO by ACS-1 in gonadal sheath cells allows transport of C17ISO-containing metabolites from somatic cells to oocytes, where they are stored until after early embryogenesis (Fig. 7).

Disruption of PL metabolism in the acs-1(RNAi)^{C17ISO} somatic gonad is a plausible mechanism underlying the Emb phenotype

PLs are major constituents of plasma membranes. Most PLs are composed of two FA acyl chains and a polar head group attached to a glycerol backbone, and PL properties strongly depend on the properties of their structural components. Alterations in PL composition potentially could have a profound influence on membrane properties and membrane-dependent cellular processes, including inter- and intracellular signaling. MS analysis revealed that wild-type and *acs-1(RNAi)^{C17ISO}* embryos had different PL compositions in a specific lipid fraction, and the changes in their levels correlated with the Emb phenotype. In wild-type samples, this fraction was composed mainly of C17ISO-containing PE (C17ISO-PE), whereas in *acs-1(RNAi)^{C17ISO}* samples, it mainly contained PL with the same acyl chain structures as in C17ISO-PE but with a yet unidentified polar head group [C17ISO-PL$^{acs\text{-}1(-)}$]. However, a reduction of C17ISO-PE per se did not correlate with Emb, suggesting that a change in PL composition or, more specifically, the enrichment in C17ISO-PL$^{acs\text{-}1(-)}$ were the key factors associated with the embryonic defect. Because low levels of C17ISO-PL$^{acs\text{-}1(-)}$ were also detected in wild-type samples, it is conceivable that they may carry out certain normal cellular functions but can negatively impact certain membrane properties when C17ISO-PEs are absent.

A direct way to examine the potential effect of C17ISO-PL$^{acs\text{-}1(-)}$ in embryos would be by feeding or injection of this lipid fraction into wild-type animals, aiming to reproduce the Emb phenotype. Feeding and microinjec-

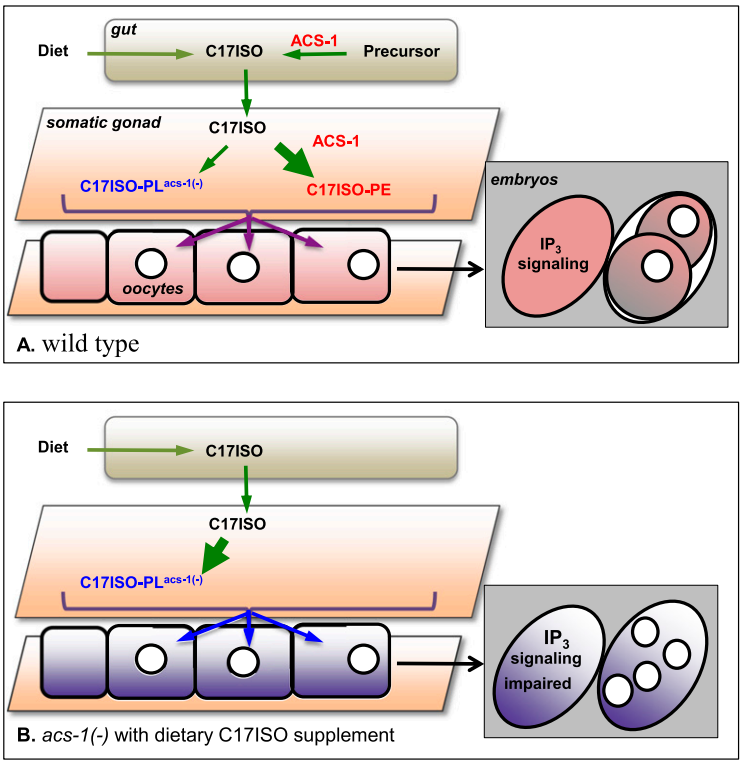

Figure 7. A model for the roles of ACS-1 in C17ISO metabolism and embryogenesis. (*A*) In wild-type animals, C17ISO is obtained from the intestine through either de novo biosynthesis or dietary absorption. In adults, C17ISO or C17ISO-containing metabolites reach oocytes by an unknown mechanism and eventually become lipid constituents in zygotes and embryos. The normal distribution of C17ISO between lipid species in wild-type embryos depends on *acs-1* expression in the somatic gonad. Activation or reactivation of C17ISO by ACS-1 directs this FA primarily into PE (C17ISO-PE), whereas activation by unidentified ACSs facilitates its incorporation into C17ISO-PL$^{acs-1(-)}$ and TAGs (Supplemental Fig. S4K). In wild type, ACS-1 competes for the C17ISO substrate to maintain a ratio between C17ISO-PE and C17ISO-PL$^{acs-1(-)}$ in favor of PE (thin vs. thick arrow) and thus prevents the dominant presence of potentially toxic C17ISO-containing lipid species. (*B*) In *acs-1(RNAi)*^{C17ISO} animals and *acs-1(lf)* mosaic animals that lack *acs-1* expression in the somatic gonad, the absence of ACS-1 activity results in the reduction of C17ISO-PE levels and an increase in C17ISO-PL$^{acs-1(-)}$ levels (thick arrow). This change in phospholipid balance, which correlates with the occurrence of the Emb phenotype, may impair IP_3 signaling or a downstream target and subsequently disrupt membrane dynamics.

tion techniques are widely used in *C. elegans* to introduce exogenous DNA and RNA. However, this approach may not be effective for introducing lipids of complex structures. Complex lipids do not freely spread between cells, but instead are delivered through highly controlled mechanisms. For example, the transport of fat from the intestine to oocytes in *C. elegans* involves specific lipid-binding proteins and receptors (Kimble and Sharrock 1983; Grant and Hirsh 1999; Hall et al. 1999; Greenstein 2005). Attempts to recapitulate the Emb phenotype in our experiments was most likely obstructed by the inability to deliver the metabolites to the right place at the right time, a common and difficult problem of targeted drug delivery. Despite this limitation, the proposed property of these C17ISO-PLs is reasonable, based on solid correlation studies, and warrants future structural and functional analysis.

Embryos affected by C17ISO-related lipid composition change are defective in plasma membrane dynamics

In *acs-1(RNAi)*^{C17ISO} embryos, an absence of any visible membrane contractions, along with their egg-filling appearance, were the earliest and the most prominent features. Several lines of evidence suggested that this phenotype was unlikely to be derived from abnormal eggshell formation that could have resulted in the swollen embryo phenotype and failed cytokinesis. First, EM analysis revealed a wild-type eggshell structure. Second, the eggshell was not sensitive to osmotic stress. Third, the establishment of A–P polarity, which depends on proper eggshell composition, was unaffected in *acs-1(RNAi)*^{C17ISO} zygotes. Finally, an observed impairment in exocytosis of GAGs, which is critical for the formation of the perivitelline space, was alone sufficient to account for the egg-filling appearance.

All features of the Emb phenotype in *acs-1(RNAi)*^{C17ISO}—including failed exocytosis of GAGs; absence of ruffling, pseudocleavage, and cleavage; and the accumulation of disordered membranous structures—indicate severe impairment of membrane dynamics. They could have resulted from changes in the physical/chemical property of the plasma membranes affecting fusion and/or fission (Bowerman and Severson 1999; Jantsch-Plunger and Glotzer 1999; Finger and White 2002; Sato et al. 2005, 2006, 2008). Remarkably, no differences in the morphology and distribution of endocytic and exocytic vesicles or ER structures were observed between wild type and *acs-1(RNAi)*^{C17ISO}, indicating that biogenesis of secretory and internalizing carriers was not, or not significantly, affected. It is conceivable to suggest that the membrane dynamics defect in *acs-1(RNAi)*^{C17ISO} embryos could be the secondary consequence of altered C17ISO-PL composition that negatively affects membrane-dependent regulatory events.

The C17ISO-PL composition changes may affect phospholipid-dependent IP_3 signaling in acs-1(RNAi)^{C17ISO} *embryos*

In *C. elegans*, IP_3 signaling is involved in multiple cellular processes from ovulation to late embryonic events (Bui and Sternberg 2002; Walker et al. 2002; Greenstein 2005; Pilipiuk et al. 2009), but its role in early embryonic stages

is less clear. An inhibition of the IP_3 pathway via overexpression of an IP_3-binding domain (i.e., a sponge) has been shown to cause mostly late embryonic lethality (Walker et al. 2002). However, a small percentage of the embryos were reported to display the phenotype similar to that associated with *acs-1(RNAi)*^{C17ISO} (egg-filling appearance, cytokinesis defects, and multinucleated blastomeres) (Walker et al. 2002). We further showed that silencing *itr-1* by RNAi causes similar erratic vesiculation of plasma membranes in early embryos and proximal gonads. These results revealed a new critical role of IP_3 signaling in membrane dynamics during pre- and post-fertilization events.

Because hyperactivity of IP_3 signaling overcomes Emb, it is reasonable to propose a model in which the *acs-1*-dependent composition of C17ISO-PL in zygotes provides optimal conditions for IP_3 signaling, which in turn regulates membrane functions during embryogenesis (Fig. 7).

Materials and methods

Terminology

(C17ISO) 15-methyl hexadecanoic acid; [*acs-1(RNAi)*^{C17ISO}] animals fed *acs-1(RNAi)* and 1 mM C17ISO in 10% DMSO (in a bacterial lawn) from the time of hatching; (C17ISO-PE) C17ISO-containing PE; [C17ISO-PL$^{acs\text{-}1(-)}$] C17ISO-containing phospholipids synthesized in the absence of *acs-1* expression.

Strains and constructs

The *acs-1(gk3066)* deletion strain obtained from the *C. elegans* Gene Knockout Consortium is homozygous-lethal. The allele contains an 800-base-pair (bp) deletion that eliminates exons 4, 5, and 6, and half of exon 7. See the Supplemental Material for more information regarding strains and plasmid constructs.

RNAi analysis and specificity of acs-1(RNAi)

All RNAi HT115 *Escherichia coli* strains were obtained from the Ahringer RNAi library (Kamath et al. 2001) except *acs-1(RNAi)*$^{56\ bp}$, which was made for this study (Supplemental Material). For all RNAi and control (HT115 *E. coli* transformed with the L4440 empty vector) experiments, eggs were released from parents by bleaching and plated on freshly prepared bacterial lawns unless otherwise specified. For the RNAi and control experiments requiring FA supplements, 450 μL of warm bacterial suspension was mixed with 50 μL of 10 mM FA in 100% DMSO per plate prior to spotting. In control plates without supplement, DMSO was mixed in bacterial suspension prior to plating at the same ratio. Since the effectiveness of RNAi may vary depending on various factors, we scored the *acs-1(RNAi)*^{C17ISO} phenotype only when we observed the L3 Sck (sick) and Lva (larval arrest) phenotypes on control *acs-1(RNAi)*^{DMSO} plates. Each experiment involving RNAi feeding was repeated at least three times.

To ensure the specificity of *acs-1(RNAi)*, the *acs-1(RNAi)* construct obtained from the RNAi library was sequenced and checked for potential secondary targets by Blast search. Two more nonoverlapping *acs-1(RNAi)* constructs targeting the *acs-1* coding sequence were made and tested by feeding (data not shown). They all reproduced the originally observed phenotypes. Temperature had no effect on the RNAi phenotypes.

Analysis of the effects of C17ISO depletion and supplementation on the *acs-1(RNAi)* phenotype, tissue-specific RNAi targeting a short sequence in the 3′ untranslated region (UTR) of *acs-1*, and tissue-specific RNAi using an *acs-1* hairpin RNA expressed under a *lim-7* promoter are described in the Supplemental Material.

GC analysis

To obtain eggs for lipid analysis, worms were washed from the plates, bleached using standard hypochlorite treatment, and monitored for egg release from corpses under microscope. When eggs were prevalent, the samples were spun down and rinsed three times in M9. The nearly dry pellets of worms or eggs were used for lipid extraction and FA methyl ester preparation, as described (Miquel and Browse 1992). This procedure does not fully eliminate carcasses of the hermaphrodites but sufficiently decreases their potential contribution to the analysis. This simpler method replaced our previous one involving separation of eggs using a sucrose gradient. The two methods generated comparable GC results. GC was performed on an HP6890N (Agilent Technologies) apparatus equipped with a DB-23 column (30 m × 250 μm × 0.25 μm) (Agilent Technologies) and flame ionization detector (FID). Each experiment was repeated at least three times.

Lipid analysis by MS

Lipid extracts were dissolved in 1 mL of methanol with 2 mM ammonium acetate and subjected to quantitative lipid analysis using a 4000 Q-Trap mass spectrometer (MDS Sciex). Samples were infused at a flow rate of 8 μL/min using a Harvard Apparatus syringe pump (Harvard Apparatus). PEs, phosphatidylserines, phosphatidylinositols, phosphatidic acid, acyl-CoAs, and phosphatidylcholines were analyzed with multiple precursor ion (PI) scans and neutral loss (NL) scans in positive and negative modes (Han and Gross 2005). PEs were also scanned with a NL scanning of *m/z* 141 in positive mode. C17-sphingosine and C17-sphinganine were identified with PI scanning of *m/z* 250 and 252 in positive mode. Fatty acyl chain identification and normal phase HPLC-MS are described in the Supplemental Material.

Other methods

Examination of the eggshell structure and osmotic response, evaluation of A–P polarity and actomyosin meshwork formation, microscopy and GFP expression analysis, reagents, and lipid extraction for MS analysis, EM analysis, RNA in situ hybridization, and immunohistochemistry are described in the Supplemental Material.

Acknowledgments

We thank Jane Hubbard, Karen Oegema, Ahna Skop, Paul Mains, William Wood, and the *Caenorhabditis* Genetics Center (CGC) for strains, and Andy Fire for vectors. We are grateful to Thomas Giddings for technical help and guidance with EM. We thank Robert Murphy, William Wood, Tom Blumenthal, Cornelia Bargmann, Thomas Cech, and our laboratory members for helpful discussions, and Aileen Sewell for editing the manuscript. The project was supported by the Howard Hughes Medical Institute, of which M.K., H.S., T.E., and M.H. are a research specialist, research associate, research technician, and investigator, respectively.

References

Abbott AL, Ducibella T. 2001. Calcium and the control of mammalian cortical granule exocytosis. *Front Biosci* **6:** D792–D806. doi: 10.2741/abbott.

Audhya A, Hyndman F, McLeod IX, Maddox AS, Yates JR III, Desai A, Oegema K. 2005. A complex containing the Sm protein CAR-1 and the RNA helicase CGH-1 is required for embryonic cytokinesis in *Caenorhabditis elegans*. *J Cell Biol* **171:** 267–279.

Baylis HA, Furuichi T, Yoshikawa F, Mikoshiba K, Sattelle DB. 1999. Inositol 1,4,5-trisphosphate receptors are strongly expressed in the nervous system, pharynx, intestine, gonad and excretory cell of *Caenorhabditis elegans* and are encoded by a single gene (itr-1). *J Mol Biol* **294:** 467–476.

Becchetti A, Whitaker M. 1997. Lithium blocks cell cycle transitions in the first cell cycles of sea urchin embryos, an effect rescued by myo-inositol. *Development* **124:** 1099–1107.

Black PN, DiRusso CC. 2007. Vectorial acylation: Linking fatty acid transport and activation to metabolic trafficking. *Novartis Found Symp* **286:** 127–138.

Bowerman B, Severson AF. 1999. Cell division: Plant-like properties of animal cell cytokinesis. *Curr Biol* **9:** R658–R660. doi: 10.1016/S0960-9822(99)80417-5.

Bui YK, Sternberg PW. 2002. *Caenorhabditis elegans* inositol 5-phosphatase homolog negatively regulates inositol 1,4,5-triphosphate signaling in ovulation. *Mol Biol Cell* **13:** 1641–1651.

Chang P, Perez-Mongiovi D, Houliston E. 1999. Organisation of *Xenopus* oocyte and egg cortices. *Microsc Res Tech* **44:** 415–429.

Clandinin TR, DeModena JA, Sternberg PW. 1998. Inositol trisphosphate mediates a RAS-independent response to LET-23 receptor tyrosine kinase activation in *C. elegans*. *Cell* **92:** 523–533.

Coleman RA, Lewin TM, Van Horn CG, Gonzalez-Barâo MR. 2002. Do long-chain acyl-CoA synthetases regulate fatty acid entry into synthetic versus degradative pathways? *J Nutr* **132:** 2123–2126.

Dal Santo P, Logan MA, Chisholm AD, Jorgensen EM. 1999. The inositol trisphosphate receptor regulates a 50-second behavioral rhythm in *C. elegans*. *Cell* **98:** 757–767.

Ellis JM, Frahm JL, Li LO, Coleman RA. 2010. Acyl-coenzyme A synthetases in metabolic control. *Curr Opin Lipidol* **21:** 212–217.

Entchev EV, Schwudke D, Zagoriy V, Matyash V, Bogdanova A, Habermann B, Zhu L, Shevchenko A, Kurzchalia TV. 2008. LET-767 is required for the production of branched chain and long chain fatty acids in *Caenorhabditis elegans*. *J Biol Chem* **283:** 17550–17560.

Finger FP, White JG. 2002. Fusion and fission: Membrane trafficking in animal cytokinesis. *Cell* **108:** 727–730.

Gönczy P, Rose LS. 2005. Asymmetric cell division and axis formation in the embryo. In *WormBook*, (ed. The *C. elegans* Research Community), *WormBook*. doi: 10.1895/wormbook.1.30.1; http://www.wormbook.org.

Grant B, Hirsh D. 1999. Receptor-mediated endocytosis in the *Caenorhabditis elegans* oocyte. *Mol Biol Cell* **10:** 4311–4326.

Green RA, Kao HL, Audhya A, Arur S, Mayers JR, Fridolfsson HN, Schulman M, Schloissnig S, Niessen S, Laband K, et al. 2011. A high-resolution *C. elegans* essential gene network based on phenotypic profiling of a complex tissue. *Cell* **145:** 470–482.

Greenstein D. 2005. Control of oocyte meiotic maturation and fertilization. In *WormBook* the online review of C elegans biology (ed. The *C. elegans* Research Community), *WormBook*. doi: 10.1895/wormbook.1.53.1; http://www.wormbook.org.

Hall DH, Winfrey VP, Blaeuer G, Hoffman LH, Furuta T, Rose KL, Hobert O, Greenstein D. 1999. Ultrastructural features of the adult hermaphrodite gonad of *Caenorhabditis elegans*: Relations between the germ line and soma. *Dev Biol* **212:** 101–123.

Han X, Gross RW. 2005. Shotgun lipidomics: Multidimensional MS analysis of cellular lipidomes. *Expert Rev Proteomics* **2:** 253–264.

Hurley JH, Meyer T. 2001. Subcellular targeting by membrane lipids. *Curr Opin Cell Biol* **13:** 146–152.

Hwang HY, Horvitz HR. 2002. The SQV-1 UDP-glucuronic acid decarboxylase and the SQV-7 nucleotide-sugar transporter may act in the Golgi apparatus to affect *Caenorhabditis elegans* vulval morphogenesis and embryonic development. *Proc Natl Acad Sci* **99:** 14218–14223.

Hwang HY, Olson SK, Esko JD, Horvitz HR. 2003. *Caenorhabditis elegans* early embryogenesis and vulval morphogenesis require chondroitin biosynthesis. *Nature* **423:** 439–443.

Jantsch-Plunger V, Glotzer M. 1999. Depletion of syntaxins in the early *Caenorhabditis elegans* embryo reveals a role for membrane fusion events in cytokinesis. *Curr Biol* **9:** 738–745.

Kahn-Kirby AH, Dantzker JL, Apicella AJ, Schafer WR, Browse J, Bargmann CI, Watts JL. 2004. Specific polyunsaturated fatty acids drive TRPV-dependent sensory signaling in vivo. *Cell* **119:** 889–900.

Kamath RS, Martinez-Campos M, Zipperlen P, Fraser AG, Ahringer J. 2001. Effectiveness of specific RNA-mediated interference through ingested double-stranded RNA in *Caenorhabditis elegans*. *Genome Biol* **2:** research0002–research0002.10. doi: 10.1186/gb-2000-2-1-research0002.

Kamath RS, Fraser AG, Dong Y, Poulin G, Durbin R, Gotta M, Kanapin A, Le Bot N, Moreno S, Sohrmann M, et al. 2003. Systematic functional analysis of the *Caenorhabditis elegans* genome using RNAi. *Nature* **421:** 231–237.

Kimble J, Sharrock WJ. 1983. Tissue-specific synthesis of yolk proteins in *Caenorhabditis elegans*. *Dev Biol* **96:** 189–196.

Kniazeva M, Crawford QT, Seiber M, Wang CY, Han M. 2004. Monomethyl branched-chain fatty acids play an essential role in *Caenorhabditis elegans* development. *PLoS Biol* **2:** e257. doi: 10.1371/journal.pbio.0020257.

Kniazeva M, Euler T, Han M. 2008. A branched-chain fatty acid is involved in post-embryonic growth control in parallel to the insulin receptor pathway and its biosynthesis is feedback-regulated in *C. elegans*. *Genes Dev* **22:** 2102–2110.

Maddox AS, Habermann B, Desai A, Oegema K. 2005. Distinct roles for two *C. elegans* anillins in the gonad and early embryo. *Development* **132:** 2837–2848.

Maddox AS, Lewellyn L, Desai A, Oegema K. 2007. Anillin and the septins promote asymmetric ingression of the cytokinetic furrow. *Dev Cell* **12:** 827–835.

Mashek DG, Li LO, Coleman RA. 2007. Long-chain acyl-CoA synthetases and fatty acid channeling. *Future Lipidol* **2:** 465–476.

Miquel M, Browse J. 1992. *Arabidopsis* mutants deficient in polyunsaturated fatty acid synthesis. Biochemical and genetic characterization of a plant oleoyl-phosphatidylcholine desaturase. *J Biol Chem* **267:** 1502–1509.

Mizuguchi S, Uyama T, Kitagawa H, Nomura KH, Dejima K, Gengyo-Ando K, Mitani S, Sugahara K, Nomura K. 2003. Chondroitin proteoglycans are involved in cell division of *Caenorhabditis elegans*. *Nature* **423:** 443–448.

Olson SK, Bishop JR, Yates JR, Oegema K, Esko JD. 2006. Identification of novel chondroitin proteoglycans in *Caenorhabditis elegans*: Embryonic cell division depends on CPG-1 and CPG-2. *J Cell Biol* **173:** 985–994.

Pilipiuk J, Lefebvre C, Wiesenfahrt T, Legouis R, Bossinger O. 2009. Increased IP3/Ca^{2+} signaling compensates depletion of LET-413/DLG-1 in *C. elegans* epithelial junction assembly. *Dev Biol* **327:** 34–47.

Poteryaev D, Squirrell JM, Campbell JM, White JG, Spang A. 2005. Involvement of the actin cytoskeleton and homotypic membrane fusion in ER dynamics in *Caenorhabditis elegans*. *Mol Biol Cell* **16:** 2139–2153.

Rappleye CA, Tagawa A, Le Bot N, Ahringer J, Aroian RV. 2003. Involvement of fatty acid pathways and cortical interaction of the pronuclear complex in *Caenorhabditis elegans* embryonic polarity. *BMC Dev Biol* **3:** 8. doi: 10.1186/1471-213X-3-8.

Riquelme CA, Magida JA, Harrison BC, Wall CE, Marr TG, Secor SM, Leinwand LA. 2011. Fatty acids identified in the Burmese python promote beneficial cardiac growth. *Science* **334:** 528–531.

Rolls MM, Hall DH, Victor M, Stelzer EH, Rapoport TA. 2002. Targeting of rough endoplasmic reticulum membrane proteins and ribosomes in invertebrate neurons. *Mol Biol Cell* **13:** 1778–1791.

Sato M, Sato K, Fonarev P, Huang CJ, Liou W, Grant BD. 2005. *Caenorhabditis elegans* RME-6 is a novel regulator of RAB-5 at the clathrin-coated pit. *Nat Cell Biol* **7:** 559–569.

Sato K, Sato M, Audhya A, Oegema K, Schweinsberg P, Grant BD. 2006. Dynamic regulation of caveolin-1 trafficking in the germ line and embryo of *Caenorhabditis elegans*. *Mol Biol Cell* **17:** 3085–3094.

Sato M, Grant BD, Harada A, Sato K. 2008. Rab11 is required for synchronous secretion of chondroitin proteoglycans after fertilization in *Caenorhabditis elegans*. *J Cell Sci* **121:** 3177–3186.

Sijen T, Fleenor J, Simmer F, Thijssen KL, Parrish S, Timmons L, Plasterk RH, Fire A. 2001. On the role of RNA amplification in dsRNA-triggered gene silencing. *Cell* **107:** 465–476.

Stricker SA. 1999. Comparative biology of calcium signaling during fertilization and egg activation in animals. *Dev Biol* **211:** 157–176.

Szafer-Glusman E, Giansanti MG, Nishihama R, Bolival B, Pringle J, Gatti M, Fuller MT. 2008. A role for very-long-chain fatty acids in furrow ingression during cytokinesis in *Drosophila* spermatocytes. *Curr Biol* **18:** 1426–1431.

Tagawa A, Rappleye CA, Aroian RV. 2001. Pod-2, along with pod-1, defines a new class of genes required for polarity in the early *Caenorhabditis elegans* embryo. *Dev Biol* **233:** 412–424.

Walker DS, Gower NJ, Ly S, Bradley GL, Baylis HA. 2002. Regulated disruption of inositol 1,4,5-trisphosphate signaling in *Caenorhabditis elegans* reveals new functions in feeding and embryogenesis. *Mol Biol Cell* **13:** 1329–1337.

Wang H, Spang A, Sullivan MA, Hryhorenko J, Hagen FK. 2005. The terminal phase of cytokinesis in the *Caenorhabditis elegans* early embryo requires protein glycosylation. *Mol Biol Cell* **16:** 4202–4213.

Watkins PA, Maiguel D, Jia Z, Pevsner J. 2007. Evidence for 26 distinct acyl-coenzyme A synthetase genes in the human genome. *J Lipid Res* **48:** 2736–2750.

Webb SE, Li WM, Miller AL. 2008. Calcium signalling during the cleavage period of zebrafish development. *Philos Trans R Soc Lond B Biol Sci* **363:** 1363–1369.

Zhang K, Kniazeva M, Han M, Li W, Yu Z, Yang Z, Li Y, Metzker ML, Allikmets R, Zack DJ, et al. 2001. A 5-bp deletion in ELOVL4 is associated with two related forms of autosomal dominant macular dystrophy. *Nat Genet* **27:** 89–93.

Zuryn S, Kuang J, Tuck A, Ebert PR. 2010. Mitochondrial dysfunction in *Caenorhabditis elegans* causes metabolic restructuring, but this is not linked to longevity. *Mech Ageing Dev* **131:** 554–561.